PROCEEDINGS OF SCIENCE

Statistical analysis into the drivers behind relativistic electron precipitation events observed by CALET on the International Space Station

A. W. Ficklin,[1,*] A. Bruno,[2,3] L. Blum,[4] G. A. de Nolfo,[2] T. G. Guzik,[1] R. Kataoka,[5,6] B. Remya[7] and S. Vidal-Luengo[4] on behalf of the CALET Collaboration

[1]*Department of Physics and Astronomy, Louisiana State University, Baton Rouge, LA, USA*
[2]*Heliophysics Science Division, NASA Goddard Space Flight Center, Greenbelt, MD, USA*
[3]*Department of Physics, Catholic University of America, Washington DC, USA*
[4]*Laboratory of Atmospheric and Space Physics, University of Colorado, Boulder, CO, USA*
[5]*National Institute of Polar Research, Tachikawa, Japan*
[6]*Department of Polar Science, SOKENDAI, Tachikawa, Japan*
[7]*Indian Institute of Geomagnetism, Navi Mumbai, India*

E-mail: aficklɜ@lsu.edu

The Calorimetric Electron Telescope (CALET), launched to the International Space Station in 2015, provides more than 7 years of continuous observation of the radiation environment at low earth orbit. Using this dataset, we present a method for the detection and categorization of MeV relativistic electron precipitation (REP) events. From this catalog we identify a subset of a few hundred REP events observed at times where CALET is in magnetic conjunction with the Van Allen probes. These conjugate measurements enable studies of associated plasma wave data from RBSPA/B and potential drivers for MeV electron precipitation. We show that roughly 10 percent of the observed REP events are associated with enhanced electromagnetic ion cyclotron wave activity, suggesting that waves can play a significant role in driving MeV electron precipitation.

38th International Cosmic Ray Conference (ICRC2023)
26 July - 3 August, 2023
Nagoya, Japan

*Speaker

PoS(ICRC2023)176

1. Introduction

The Calorimetric Electron Telescope (CALET) [1], launched to the International Space Station in 2015, provides more than 7 years of observation of the radiation environment at low earth orbit (LEO). Although the primary scientific goals of CALET is the observation of cosmic rays from a few GeV up to 1 PeV, it was shown early on in the CALET mission that the upper layers of CALET were sensitive to much lower energy (>1 MeV) radiation events, namely relativistic electron precipitation (REP) events [2][13]. These REP events occur when trapped or quasi-trapped electrons in the outer radiation belt are scattered into the loss cone and are subsequently lost to the upper atmosphere [3] [4], leading to the depletion of the outer radiation belt and increased bursts of radiation at LEO and into the upper atmosphere. Although several spacecraft, such as the Solar, Anomalous, and Magnetospheric Particle Explorer (SAMPEX), have observed REP events for several decades[12], the drivers behind these events are not fully understood. One of the more commonly accepted drivers of electron precipitation is pitch angle scattering due to wave-particle interactions with plasma waves in the magnetosphere, namely Electromagnetic Ion Cyclotron (EMIC) waves that have been identified as potential drivers of >1 MeV electrons [5]. This work looks to investigate this potential driver by comparing REP events observed by CALET to EMIC wave events observed by the Radiation Belt Storm Probes (RBSP) to find the frequency at which REP events occur in close proximity with EMIC wave activity.

2. Data Analysis

2.1 REP Event Catalog

CALET was launched in August 2015 to the International Space Station (ISS) for the primary purpose of directly measuring the cosmic-ray total electron spectrum up to energies of tens of TeV. The CALET calorimeter (CAL), shown in Figure 1, has a depth of 30 radiation lengths (X_0) at normal incidence and includes three separate sub-detectors. The Charge Detector (CHD) consists of two layers of 14 plastic scintillating paddles and can measure the charge of nuclei up to Z = 40. The Imaging Calorimeter (IMC) contains 16 layers of 448 scintillating fibers each which provide accurate tracking for most events. Most of the shower energy is deposited in the Total Absorption Calorimeter (TASC), with 12 layers of 16 PWO logs that can contain electromagnetic showers up to TeV energies. For REP event observations we utilize the count rates of the two layers of the CHD, CHDX and CHDY, which are sensitive to >1.6 MeV and >3.6 MeV electrons respectively.

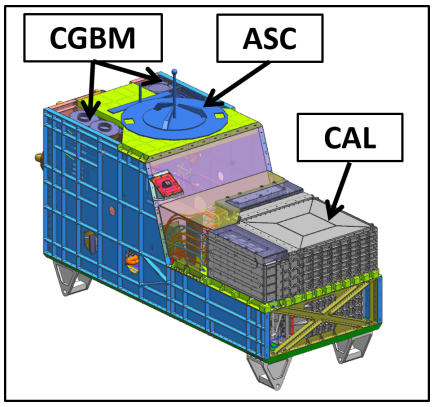

Figure 1: CALET structure indicating the CALET Gamma-ray Burst Monitor (CGBM), Advanced Stellar Compass (ASC), and calorimeter (CAL).

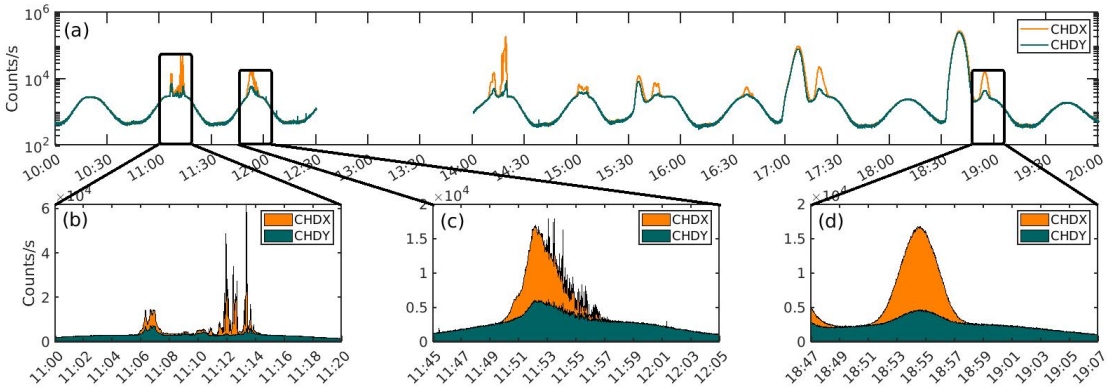

Figure 2: *(a)* Count rates of the CHDX and CHDY for a 10 hour period exhibiting types of precipitation observations. *(b)* An example of an event classified by the SOM as rapid precipitation. *(c)* An example of an event classified as a mixed between rapid and smooth precipitation. *(d)* An example of an event classified as smooth precipitation.

The REP event catalog was produced by S. Vidal-Luengo et al.(2023)[6] using a an algorithm that leverages self organizing maps (SOM) to automatically detect and sort REP events in the CALET dataset. The algorithm first calculates the power spectral density (PSD) for every 10 minute window of data from October 2015 to October 2021 and feeds this into the SOM. The SOM then sorts the PSDs for each window into groups with similar characteristics, getting sorted into three categories, rapid precipitation, smooth precipitation, and noise. Events classified as noise are simply background count rates and are removed from the catalog, while events classified as smooth precipitation are considered to be due primarily to trapped or quasi-trapped particles and not the REP events we are interested in for this analysis. Figure 2 shows an example of a rapid precipitation and smooth precipitation events, as well as an event that contains feature of both types.

Excluding events classified as noise, a total of 22,749 events were identified, with their spatial distribution in magnetic local time (MLT) and McIlwain L shell parameter (L) shown in the left panel of Figure 3. The events are shown to be distributed evenly in MLT but show a strong dependence on L shell with most events being between L = 3 and L = 5. With the smooth events neglected, a total of 1448 rapid precipitation events remain, and are the events most likely associated with true REP events. The spatial distribution of these events, shown in the right panel of Figure 3, now reveals a strong dependence on MLT and L shell. Of particular interest is the increased population of events in the pre-midnight sector where enhanced EMIC wave activity is expected [8].

2.2 EMIC Wave Event Catalog

The EMIC wave events used in this work were pulled from a catalog of events produced by B. Remya (2023)[7] which uses data from the Electric and Magnetic Field Instrument Suite and Integrated Science (EMFISIS) aboard the Radiation Belt Science Probes (RBSP-A/B). The EMFISIS instrument[10] measures electric and magnetic field wave data covering frequencies from 1Hz to 400kHz and its data includes calculated power spectrum density that can be used to identify several different types of plasma wave activity. For the detection of the EMIC wave events used

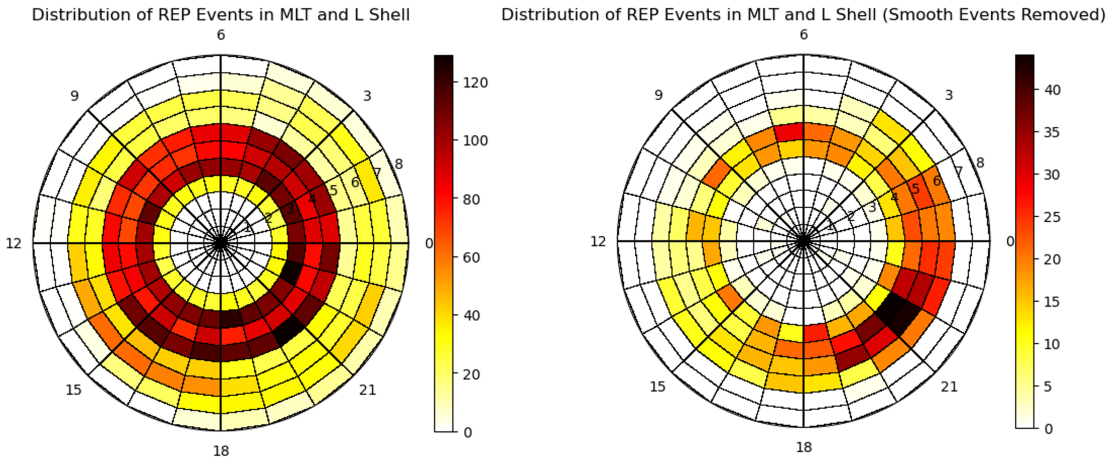

Figure 3: Spatial distribution of smooth precipitation (left) events and rapid precipitation (right) events in MLT and L.

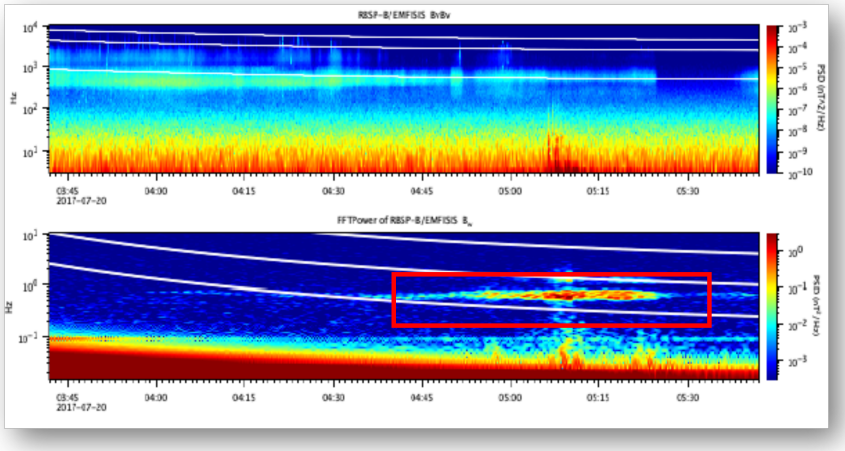

Figure 4: Magnetic field waveform measured by RBSP for a period with enhanced EMIC wave activity, shown in the red box.

in this analysis, an automatic wave detection algorithm J. Bortnik (2006)[9] was used to identify events in the desired frequency of 0.5 - 5Hz. The algorithm selects events based on their spectral peak and requires the peak to be one order higher than the calculated background for a one hour period surrounding the potential event. In total, 664 events were identified in RBSP-A data and 443 events for RBSP-B. Figure 4 shows an example of enhanced EMIC wave activity that was identified and included in the event catalog. Additionally, Figure 5 shows the spatial distribution of the EMIC wave events identified which reveals a enhanced population of events in the pre-midnight and pre-noon sectors.

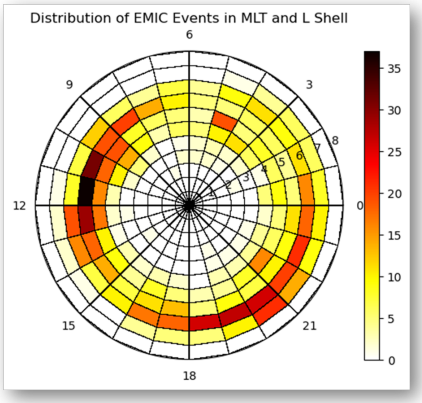

Figure 5: Spatial distribution of EMIC wave events in MLT and L Shell.

2.3 Checking for Coincidence

In order to appropriately compare the events included in these two catalogs, geomagnetic information was calculated for all events using the latest IGRF 13[14] internal magnetic field model and Tsyganenko 05[15] external field model. Then, on an event by event basis, events were checked for coincidence in time, as well as spatially using their geomagnetic location in MLT and L shell. The initial criteria for coincidence were as follows:

$$L_{CAL-min} - 0.5RE < L_{RBSP} < L_{CAL-max} + 0.5RE, \tag{1}$$

$$MLT_{CAL-min} - 1h < MLT_{RBSP} < MLT_{CAL-max} + 1h, \tag{2}$$

$$T_{CAL-start} - 10min < T_{RBSP} < L_{CAL-stop} + 10min, \tag{3}$$

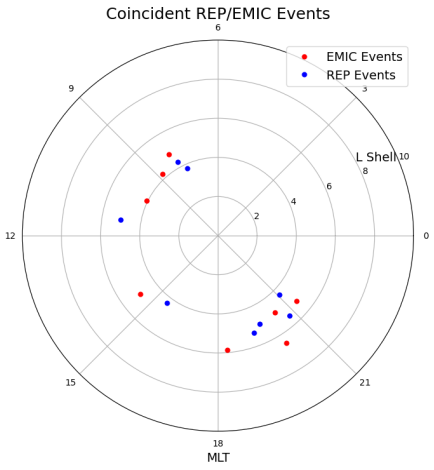

Figure 6: Spatial distribution of coincident REP/EMIC wave events in MLT and L.

With these conditions applied, 78 REP events out of 1448 were found to be coincident in both time and space with either RBSP-A or RBSP-B regardless of EMIC wave activity, while 8 events were coincident with either probe during EMIC wave activity. This result shows that, with this initial criteria, 10 percent of REP events are coincident with EMIC wave activity. When these events are viewed spatially, shown in Figure 6, a clear anisotropy is revealed showing the majority of the coincident events being focused in the pre-midnight and pre-noon sectors.

To view how dependent on MLT and L shell these statistics are, the analysis was repeated for a grid of MLT and L shell criteria up

to +/- 5 hours in MLT and +/- 5 in L shell, but with the same +/- 10 minute window in time. The results, shown in Figure 7, show how the number of coincident events change as the criteria is relaxed in either MLT or L shell. The number of coincident events shows a stronger dependence on the criteria applied to MLT, which could be beneficial since recent work suggests that EMIC wave events can be wider in MLT than the initial coincidence criteria implies[11].

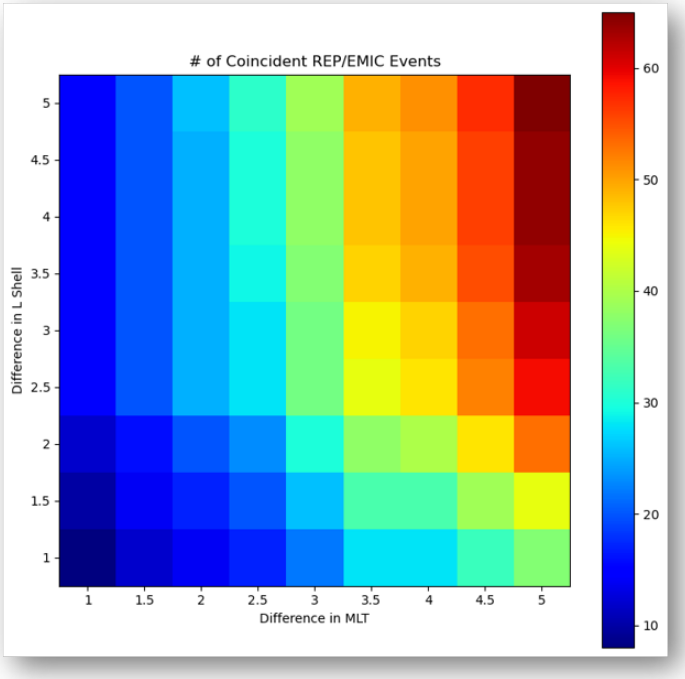

Figure 7: Number of coincident REP/EMIC wave events as a function of MLT and L shell.

3. Conclusions

The analysis presented in this work looked to find evidence that EMIC wave activity is a significant driver of REP events. Using a catalog of REP events observed by CALET and EMIC wave events observed by RBSP, we found that around 10 percent of REP events are coincident with EMIC wave activity, implying that they do play a part in driving these radiation belt loss events. Additionally, we found that both the EMIC wave events and REP events show a clear asymmetry in terms of MLT and L shell, with both populations showing a clustering of events in the pre-midnight sector.

Acknowledgements

We gratefully acknowledge JAXA's contributions to the development of CALET and to the operations onboard the International Space Station. The CALET effort in Italy is supported by ASI under Agreement No. 2013- 018-R.0 and its amendments. The CALET effort in the United States is supported by NASA through Grants No. 80NSSC20K0397, No. 80NSSC20K0399, and

No. NNH18ZDA001N-APRA18-0004. This work is supported in part by JSPS Grant-in- Aid for Scientific Research (S) Grant No. 19H05608 in Japan.

References

[1] S. Torii for the CALET Collaboration, *"Highlights from the CALET observations for 7.5 years on the International Space Station,"* in *Proceedings of Science (ICRC2023; this conference)*, (2023).

[2] R. Kataoka et al., *Relativistic Electron Precipitation at International Space Station: Space Weather Monitoring by Calorimetric Electron Telescope.,* in *Geophysical Research Letters*,43 (9), 4119-4125. (2016), doi: https://doi.org/10.1002/2016GL068930.

[3] Y. Shprits et al., *Controlling effect of the pitch angle scattering rates near the edge of the loss cone on electron lifetimes.*, in *Journal of Geophysical Research: Space Physics*, 111(A12), (2006).

[4] R. Millan and R. Thorne, *Review of radiation belt relativistic electron losses*, in *Journal of Atmospheric and Solar-Terrestrial Physics* 69 (3), 362–377, (2007).

[5] R. Thorne and C. Kimmel, *Relativistic electron precipitation during magnetic storm main phase*, in *Journal of Geophysical Research* 76 (19), 4446–4453, (1971).

[6] S. Vidal-Luengo et al., *Characterization of Relativistic Electron Precipitation Events Observed by the CALET Experiment Using Self-Organizing-Maps*, To Be Submitted, (2023).

[7] B. Remya et al., *Understanding Quiet and Storm Time EMIC Waves - Van Allen Probes Results*, Submitted to JGR: Space Physics, (2023).

[8] K. Sigsbee, CA Kletzing, J. Faden, CW. Smith, *Occurrence Rates of Electromagnetic Ion Cyclotron (EMIC) Waves With Rising Tones in the Van Allen Probes Data Set*. JGR: Space Phys. Feb;128(2), doi: 10.1029/2022JA030548. (2023)

[9] J. Bortnik et al., *An automatic wave detection algorithm applied to Pc1 pulsations*, Journal of Geophysical Research, 112, A04204, (2006).

[10] CA Kletzing et al. *The electric and magnetic field instrument suite and integrated science (emfisis) on rbsp.*, Space Science Review, 179, 127. doi: 10.1007/s11214-013-9993-6 (2013)

[11] L Blum et al. *On the spatial and temporal evolution of EMIC wave-driven MeV electron precipitation*, To be submitted. (2023).

[12] R. Nakamura et al. *Relativistic electron precipitation enhancements near the outer edge of the radiation belt*, Geophysical Research Letters, 22 (9), 1129–1132, (1995).

[13] A. Bruno et al. *EMIC-Wave Driven Electron Precipitation Observed by CALET on the International Space Station*, Geophysical Research Letters, 49 (6), (2022)

[14] P. Alken et al. *International geomagnetic reference field: the thirteenth generation.* Earth Planet Sp, 73, 49, (2021)

[15] N.A. Tsyganenko and M.I. Sitnov *Modeling the dynamics of the inner magnetosphere during strong geomagnetic storms.* Journal of Geophysical Research: Space Physics, 110(A3), (2005)

Full Author List: CALET Collaboration

O. Adriani[1,2], Y. Akaike[3,4], K. Asano[5], Y. Asaoka[5], E. Berti[2,6], G. Bigongiari[7,8], W.R. Binns[9], M. Bongi[1,2], P. Brogi[7,8], A. Bruno[10], N. Cannady[11,12,13], G. Castellini[6], C. Checchia[7,8], M.L. Cherry[14], G. Collazuol[15,16], G.A. de Nolfo[10], K. Ebisawa[17], A.W. Ficklin[14], H. Fuke[17], S. Gonzi[1,2,6], T.G. Guzik[14], T. Hams[11], K. Hibino[18], M. Ichimura[19], K. Ioka[20], W. Ishizaki[5], M.H. Israel[9], K. Kasahara[21], J. Kataoka[22], R. Kataoka[23], Y. Katayose[24], C. Kato[25], N. Kawanaka[20], Y. Kawakubo[14], K. Kobayashi[3,4], K. Kohri[26], H.S. Krawczynski[9], J.F. Krizmanic[12], P. Maestro[7,8], P.S. Marrocchesi[7,8], A.M. Messineo[8,27], J.W. Mitchell[12], S. Miyake[28], A.A. Moiseev[29,12,13], M. Mori[30], N. Mori[2], H.M. Motz[31], K. Munakata[25], S. Nakahira[17], J. Nishimura[17], S. Okuno[18], J.F. Ormes[32], S. Ozawa[33], L. Pacini[2,6], P. Papini[2], B.F. Rauch[9], S.B. Ricciarini[2,6], K. Sakai[11,12,13], T. Sakamoto[34], M. Sasaki[29,12,13], Y. Shimizu[18], A. Shiomi[35], P. Spillantini[1], F. Stolzi[7,8], S. Sugita[34], A. Sulaj[7,8], M. Takita[5], T. Tamura[18], T. Terasawa[5], S. Torii[3], Y. Tsunesada[36,37], Y. Uchihori[38], E. Vannuccini[2], J.P. Wefel[14], K. Yamaoka[39], S. Yanagita[40], A. Yoshida[34], K. Yoshida[21], and W.V. Zober[9]

[1]Department of Physics, University of Florence, Via Sansone, 1 - 50019, Sesto Fiorentino, Italy, [2]INFN Sezione di Firenze, Via Sansone, 1 - 50019, Sesto Fiorentino, Italy, [3]Waseda Research Institute for Science and Engineering, Waseda University, 17 Kikuicho, Shinjuku, Tokyo 162-0044, Japan, [4]JEM Utilization Center, Human Spaceflight Technology Directorate, Japan Aerospace Exploration Agency, 2-1-1 Sengen, Tsukuba, Ibaraki 305-8505, Japan, [5]Institute for Cosmic Ray Research, The University of Tokyo, 5-1-5 Kashiwa-no-Ha, Kashiwa, Chiba 277-8582, Japan, [6]Institute of Applied Physics (IFAC), National Research Council (CNR), Via Madonna del Piano, 10, 50019, Sesto Fiorentino, Italy, [7]Department of Physical Sciences, Earth and Environment, University of Siena, via Roma 56, 53100 Siena, Italy, [8]INFN Sezione di Pisa, Polo Fibonacci, Largo B. Pontecorvo, 3 - 56127 Pisa, Italy, [9]Department of Physics and McDonnell Center for the Space Sciences, Washington University, One Brookings Drive, St. Louis, Missouri 63130-4899, USA, [10]Heliospheric Physics Laboratory, NASA/GSFC, Greenbelt, Maryland 20771, USA, [11]Center for Space Sciences and Technology, University of Maryland, Baltimore County, 1000 Hilltop Circle, Baltimore, Maryland 21250, USA, [12]Astroparticle Physics Laboratory, NASA/GSFC, Greenbelt, Maryland 20771, USA, [13]Center for Research and Exploration in Space Sciences and Technology, NASA/GSFC, Greenbelt, Maryland 20771, USA, [14]Department of Physics and Astronomy, Louisiana State University, 202 Nicholson Hall, Baton Rouge, Louisiana 70803, USA, [15]Department of Physics and Astronomy, University of Padova, Via Marzolo, 8, 35131 Padova, Italy, [16]INFN Sezione di Padova, Via Marzolo, 8, 35131 Padova, Italy, [17]Institute of Space and Astronautical Science, Japan Aerospace Exploration Agency, 3-1-1 Yoshinodai, Chuo, Sagamihara, Kanagawa 252-5210, Japan, [18]Kanagawa University, 3-27-1 Rokkakubashi, Kanagawa, Yokohama, Kanagawa 221-8686, Japan, [19]Faculty of Science and Technology, Graduate School of Science and Technology, Hirosaki University, 3, Bunkyo, Hirosaki, Aomori 036-8561, Japan, [20]Yukawa Institute for Theoretical Physics, Kyoto University, Kitashirakawa Oiwake-cho, Sakyo-ku, Kyoto, 606-8502, Japan, [21]Department of Electronic Information Systems, Shibaura Institute of Technology, 307 Fukasaku, Minuma, Saitama 337-8570, Japan, [22]School of Advanced Science and Engineering, Waseda University, 3-4-1 Okubo, Shinjuku, Tokyo 169-8555, Japan, [23]National Institute of Polar Research, 10-3, Midori-cho, Tachikawa, Tokyo 190-8518, Japan, [24]Faculty of Engineering, Division of Intelligent Systems Engineering, Yokohama National University, 79-5 Tokiwadai, Hodogaya, Yokohama 240-8501, Japan, [25]Faculty of Science, Shinshu University, 3-1-1 Asahi, Matsumoto, Nagano 390-8621, Japan, [26]Institute of Particle and Nuclear Studies, High Energy Accelerator Research Organization, 1-1 Oho, Tsukuba, Ibaraki, 305-0801, Japan, [27]University of Pisa, Polo Fibonacci, Largo B. Pontecorvo, 3 - 56127 Pisa, Italy, [28]Department of Electrical and Electronic Systems Engineering, National Institute of Technology (KOSEN), Ibaraki College, 866 Nakane, Hitachinaka, Ibaraki 312-8508, Japan, [29]Department of Astronomy, University of Maryland, College Park, Maryland 20742, USA, [30]Department of Physical Sciences, College of Science and Engineering, Ritsumeikan University, Shiga 525-8577, Japan, [31]Faculty of Science and Engineering, Global Center for Science and Engineering, Waseda University, 3-4-1 Okubo, Shinjuku, Tokyo 169-8555, Japan, [32]Department of Physics and Astronomy, University of Denver, Physics Building, Room 211, 2112 East Wesley Avenue, Denver, Colorado 80208-6900, USA, [33]Quantum ICT Advanced Development Center, National Institute of Information and Communications Technology, 4-2-1 Nukui-Kitamachi, Koganei, Tokyo 184-8795, Japan, [34]College of Science and Engineering, Department of Physics and Mathematics, Aoyama Gakuin University, 5-10-1 Fuchinobe, Chuo, Sagamihara, Kanagawa 252-5258, Japan, [35]College of Industrial Technology, Nihon University, 1-2-1 Izumi, Narashino, Chiba 275-8575, Japan, [36]Graduate School of Science, Osaka Metropolitan University, Sugimoto, Sumiyoshi, Osaka 558-8585, Japan, [37]Nambu Yoichiro Institute for Theoretical and Experimental Physics, Osaka Metropolitan University, Sugimoto, Sumiyoshi, Osaka 558-8585, Japan, [38]National Institutes for Quantum and Radiation Science and Technology, 4-9-1 Anagawa, Inage, Chiba 263-8555, Japan, [39]Nagoya University, Furo, Chikusa, Nagoya 464-8601, Japan, [40]College of Science, Ibaraki University, 2-1-1 Bunkyo, Mito, Ibaraki 310-8512, Japan

PoS(ICRC2023)176